Nature of motions between sarcomeres in asynchronously contracting cardiac muscle cells

John W. Krueger, Adam Denton, and Gerard Siciliano
The Albert Einstein College of Medicine, Bronx, New York 10461

ABSTRACT We observed the asynchronized motions that occur between the sarcomeres during spontaneous contractions to study the mechanical nature of the intact cardiac muscle cell (guinea pig, rat). The cell's striated image is detected by a photodiode array, and sarcomere length is measured very precisely 526/s in two separate, selected fixed regions of the image from the localized frequency of the array's video signal (Krueger and Denton, 1992, *Biophys. J.*, 61:129–144, second of two companion manuscripts). An extension of this approach is described here in which the spatial variation of sarcomere length is visualized by scanned sampling, i.e., displacing the first window along the length of the cell, and nonuniform strain is deduced from the histograms of sarcomere length. The nature of asynchronous motion that was obtained from both fixed sampling of the sarcomere's dynamics and by scanned sampling of sarcomere length was consistent. In spontaneously active cells, sarcomeres lengthen ~0.1 μm beyond their rest length before the arrival of the propagated wave of contraction. Such prelengthening extends in a nonuniform fashion for ~ 10 to 15 μm in the unattached cell. Shortening and lengthening motions, being in proportion for both large and small displacements, are well coupled. Lifting the cell from the substrate showed that the force that sustains prelengthening arises within the cell. Differences in the sarcomere's dynamics in synchronous and asynchronous contractions corroborate that asynchrony imposes an additional internal restoring force. The extra force estimated to account for prelengthening (0.5–0.7 mN/mm^2) has little effect on the velocity of shortening, and so the true intracellular restoring force must be correspondingly larger. The intracellular restoring force may contribute significantly to the rapid 'diastolic' recoil of the heart muscle at short sarcomere lengths.

INTRODUCTION

Asynchronous waves of spontaneous shortening in the isolated cardiac muscle cell reveals nonuniform distribution of myoplasmic calcium (24), but the nature of the motions must also reflect the mechanical connections between sarcomeres. Asynchrony can be detected by diffraction (13), inferred by regional differences in light transmission (3), or detected by differential patterns of displacement at each end of the cell (1). None of these methods can be used to measure the motions between sarcomeres. The motions of individual striations can be followed by computer-based video imaging (16, 20, 22), but this approach would prove cumbersome for sampling spontaneous events at the temporal resolution required in most experiments.

A companion study (10) describes a method to evaluate the uniformity of contraction in isolated heart cells. Sarcomere length is sampled simultaneously in two independent, selected regions of the image to quantify the dynamics of local shortening. This report uses an additional feature to map the nonuniform distribution of sarcomere length by displacing the region of sampling in a controlled fashion along the cell. By eliminating any systematic effect of contractile translation upon sampling at a fixed region, scanning provides an interpretation of asynchronous motion that is independent of the dynamics of specific striations.

The isolated cardiac cell relengthens vigorously (8, 13, 14), and a steady restoring force can be measured in the isolated cardiac myofibril (4) or cell (7) that has been shortened to below its rest length. The contribution of the cellular relengthening force to the restoring force in isolated heart muscle is unclear, however, largely because the former has not been measured in physiologically intact cells. We show here that the asynchronous motions between sarcomeres provides a way to estimate the magnitude of the internal restoring force in the intact cell. The simplest interpretation of the nonuniform patterns of strain we find requires a parallel elastic element that is not tethered to contiguous sarcomeres. Such long range attachments might impart an organization to the striations (10) and/or constitute a simple way for the cell to sense a change in its mechanical environment.

Preliminary reports of this technique have been described elsewhere (8, 11).

Address correspondence to Dr. John W. Krueger, Department of Physiology & Biophysics, Albert Einstein College of Medicine, Bronx, NY 10461.
Mr. Denton's current address is AT&T Bell Laboratories, Middletown, NJ 07748.

0006-3495/92/01/145/16 $2.00

METHODS

Single cardiac cells were isolated enzymatically from the ventricular myocardium as described previously (Rat, 13; Guinea Pig, 15). The experimental solutions, the conditions of study, and the microscopy and experimental arrangement are described in a companion article (10), and so only the features essential to this report will be described.

Mapping of the distribution of sarcomere motions by FM detection

Sarcomere length was sampled 526/s at two independently selected sites on the cell by an extension of the phase-locked loop method (10, 18). In one mode of observation, each position of sampling remains fixed to measure nearly simultaneously the contractile dynamics in different areas of the cell. Fig. 1 shows additional circuitry that automatically displaces the first sampling interval (window 1), narrowed to sample ~2 striations, along the length of the cell. The scanning method displays the sarcomere length as a function of position throughout the cell, as shown in Fig. 2, and which was applied to visualize the static patterns of the variation in sarcomere length (10). The scanning mode also provides information about the mechanics of asynchrony that does not rely on the sampling of specific elements.

The additional features of the circuit that enable scanned sampling are enclosed in the dashed area in Fig. 1. The principal components are a voltage-controlled monostable multivibrator, a ramp generator, and a summation amplifier. The delay monostable multivibrator for window 1 has been modified to produce a time delay that is proportional to an applied control voltage. This voltage is obtained as the algebraic sum of the ramp generator output and the POSITION 1 control, which is connected as a variable voltage divider. Initially, the ramp generator is in a rest state in which its output is zero volts. The position of window 1 is therefore determined only by the POSITION 1 control. The ramp generator remains in the rest state until it is triggered into operation by a received "START SWEEP" pulse. Once the ramp generator has been triggered, its output voltage rises linearly in time. This rising voltage adds to the delay control voltage, increasing the delay period of the monostable multivibrator governing the position of window 1. The result is that the first window migrates across the cell as the output of the ramp generator rises. The starting position of the window (window 1) is adjustable, being determined by the setting of the POSITION 1 control.

The length of the sweep which displaces window 1 is controlled by the position of window 2, and the latter is always positioned to the right of the starting position of window 1. When the two windows superimpose a coincidence detector circuit outputs a RESET pulse to the ramp generator, resetting the ramp generator to its initial state and returning its output voltage to zero. This returns window 1 to its initial (leftmost) position, where it remains until the ramp generator is again triggered by a START SWEEP pulse. Consequently, the rate of repeated scanning of the cell is inversely related to the separation of the windows. A length of the cell 45 μm long is scanned 16/s, and this is increased to 60/s by reducing the separation of the windows to 12 μm. With each computation, the position of the sample window is

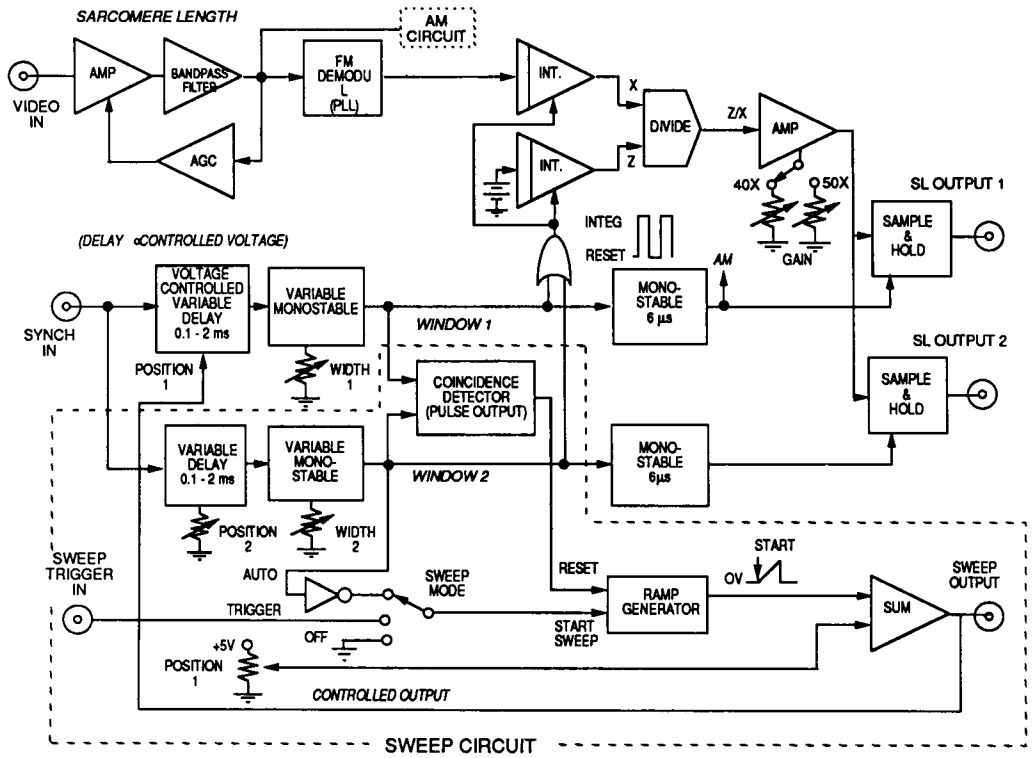

FIGURE 1 Schematic diagram of the method for the detection nonuniform motion between sarcomeres by scanning the point of sampling. The dashed area includes the sweep circuit for scanned sampling. Refer to text for circuit description. *AMP,* amplifier; *PLL,* phase locked-loop; *INT,* integrator; *AGC,* automatic gain control; *DIV,* divider; *SUM,* summing amplifier; AM CIRCUIT refers to additional components shown in Fig. 2, reference 10.

advanced 1.2 μm, a value that is determined by the ratio of the scan period of the photodiode array (1.9 ms) and the rate of rise of the ramp generator which displaces the first window. The spatial resolution for each sarcomere length computation is determined simply from the width of the first window, the minimum value of which is 2.0 μm. The calibration of the device and sampling of the striations is discussed in the companion article (10).

A three-way sweep mode switch allows the sweep function to be controlled in various ways. When the switch is in the TRIGGER position, the START SWEEP input of the ramp generator is controlled by an external device; a single sweep occurs whenever a pulse is received. When the SWEEP MODE switch is in the AUTO position, the ramp generator is connected to the window 2 signal, which continuously triggers the sweep function, once per scan line. Once triggered, the ramp generator ignores any extra START SWEEP pulses until it has returned to its rest state. Therefore, the continuous START SWEEP pulses have no effect until a sweep has been completed or the ramp generator has been reset, at which point it is soon triggered again and another sweep begins. The connection of START SWEEP to the window 2 signal instead of SYNC ensures that a new sweep does not begin until exactly one scan-line period after the previous sweep has ended. The SWEEP MODE switch also includes an OFF position which connects the ramp generator START SWEEP input to ground, preventing the ramp generator from triggering. This disables the sweep function; the position of window 1 is then determined only by the setting of the POSITION 1 control.

Resolution and interpretation of nonuniformity

A precision nonuniform test grating demonstrated that the method accurately resolves a predetermined step change in the spacing of contiguous striations as small as 0.10 μm to ±0.01 μm over a 2.4 μm displacement of the sampling window that requires two computations (cf. 10; Fig. 3). However, for the purpose of assessing nonuniform motions we also considered the circuit's response to the maximum gradient of nonuniformity expected. Using the minimum width for the scanning window of 2.0 μm, the transition for a step change in striation spacing from 2.00 to 3.00 μm was completed within three computations. Because each computation represents an advancement of the window by 1.2 μm on the cell, the method should detect any gradient of striation spacing which is $< \pm 1.00$ μm/(3 × 1.2 μm), or a value equivalent to a sudden change equal to 30% the length of the sarcomere. Because the functional range of the cardiac sarcomere spans a range of ~ ±25% of its rest length, the method should resolve the scale of any nonuniform sarcomere motions that might reasonably be expected to occur. Because sarcomere length represents the running average between two striations, precision is less when a discrete isolated fluctuation in length occurs. This event, however, gives rise to characteristic changes in the sarcomere length histogram (cf. 10; Fig. 4).

RESULTS

Some general features of asynchronous contractions in isolated myocytes

Shortening and relengthening were well synchronized when contraction was triggered by electrical stimulation (10). When myoplasmic calcium is elevated, guinea pig myocytes shorten spontaneously and asynchronously (24), and the initial sarcomere length may be shortened (23). The spontaneous behavior has been well described in the literature, and it is characterized by a small focus of shortening and relengthening that encompasses only a few sarcomeres and propagates in a wave-like fashion as diagramed in Fig. 2 *A*. The spatial nature of asynchronous activity is difficult to study with prior imaging methods, because its spontaneous nature would overburden data sampling at adequate temporal resolutions.

Fig. 2 further demonstrates application of the circuit to display the pattern of asynchronous sarcomere length changes on a cathode ray tube (CRT). The distribution of the sarcomere length along the length of an scanned segment on the cell is displayed as a horizontal raster whose intensity is modulated by the sarcomere length. The raster is displaced downward with time, so that the resulting two-dimensional pattern of the bright and dark regions correspond to segments mapped on the cell where sarcomere length is longer or shorter, respectively. This provides a convenient way to examine several features of asynchronous activity, as shown in Fig. 2, *B* and *C*. For example, it is well known that spontaneous activity arises most often near the end of the cell, but the display also shows that it may or may not propagate throughout the cell (cf. 2nd contraction, Fig. 2 *B*). In the next spontaneous contraction, two independent foci enter the scanned field from opposite ends of the cell and fail to propagate beyond their point of collision (cf. 3rd contraction, Fig. 2 *B*). Comparable displays recorded from other cells indicate that the velocity of propagation may be constant, it may increase, or it may decrease during the course of any spontaneous contraction. The average velocity of propagation for the contractile waves measured by this simple manner in 6 rat cells was 82.3 ± 27 μm/s (27 occurrences) and is in accord with previous reports (3, 20, 16) and also for propagation of calcium waves in guinea pig myocytes (24). However, the velocity of propagation of the contractile waves can vary appreciably in different spontaneous beats. These results demonstrate that the fate of any contractile wave is highly variable, and so the propagation of the focus of the contractile wave does not involve an unconstrained positive feedback mechanism.

1. Patterns of asynchronous motions. Areas of brightening in the scanned raster displays that are illustrated in Fig. 2 can be unambiguously associated with longer sarcomeres. (The periodic brightening indicates patches where sarcomere length is relatively uniform [cf. 10]). Examined at higher temporal resolution, individual rasters in these displays demonstrate also that areas of lengthening precede the contractile focus as shown in Fig. 2 *C*, and that this 'prelengthening' does not occur simultaneously throughout the length of the cell. These displays directly support inferences about lengthening

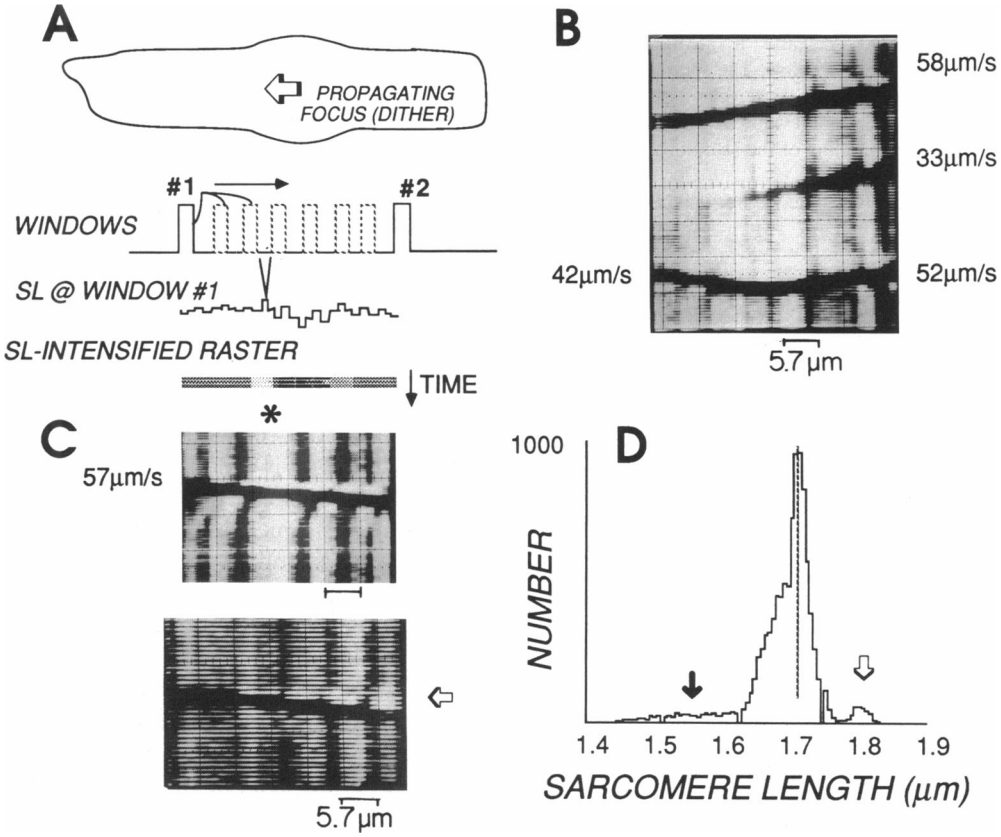

FIGURE 2 Method for mapping the distribution of sarcomere motions during contraction. (*A*) Multiple images of the first window (#1) denote its displacement in 1.2 μm steps along the cell from left to right. The allowable range for scanning is determined by the initial setting for the first window and the fixed position of the second window (#2). The striation spacing in each window is computed >500/s from the average value of the FM demodulated signal that is selected by the respective window's width and current position. The sarcomere length sampled in window #1 is used to modulate the intensity of a raster line that it is displaced downward with time on a storage oscilloscope. This creates a two-dimensional representation of the sarcomere motions in the spontaneously contracting cell. (*B* and *C*) Two-dimensional 'raster' display of asynchronized sarcomere motions within the cell. Brighter and darker areas represent regions of longer or shorter sarcomeres, respectively. Broad arrow in the lower panel of *C* denotes a bright region indicating an area of sarcomere lengthening that precedes the darker wave of contraction which advances at 103 μm/s. Asterisk denotes patches in which sarcomere length is uniform (cf. 10). Horizontal calibration, 5.7 μm/divider. Vertical bands in *B* and *C* reveal patches of sarcomeres that are more uniform in length, and the numbers refer to the velocity of propagation. (*D*) Histogram obtained by computer sampling of the sarcomere lengths obtained by scanning a spontaneously contracting myocyte (rat). The central component of the histograms appear broadened in an asymmetric fashion, and the additional components at the extremes denote sarcomere lengthening (*open arrow*) and shortening (*solid arrow*).

drawn from changes of light transmission in isolated cells (3), but they additionally reveal the instantaneous distribution of prelengthening. For example, inspection of the original photographs showed that both the degree and the extent of this brightening appeared to increase with the advance of the contractile wave, and that the area of lengthening extends nonuniformly for 10 to 15 μm (Fig. 2 *C*, *bottom*).

The two-dimensional display provides a qualitative map of asynchronous contractile motion in the cell, but because of the evident difficulty in recording intensity of the display other approaches are required to measure sarcomere length. Sarcomere length was sampled continuously in the repetitively scanned segments of the spontaneously contracting cell by a microcomputer. A representative histogram showing the distribution of sarcomere length in a spontaneously contracting cell is shown in Fig. 2 *D*. The histogram shows a clear component representing the increase in the incidence of striations that are shorter than the initial 'rest' length as expected, but it also indicates that asynchronous shortening results in sarcomeres that were ~0.1 μm longer than the rest length (Fig. 2 *D*). Most often the distribution of sarcomere shortening was fairly broad and without notable feature as illustrated in Figs. 2 *D* and 3 *A*. Occasionally, however, histograms were seen with dis-

crete components in sarcomere shortening (Fig. 3 *B*) that could not be attributed to the isolated peaks or dropouts in the display that arise from interactions between sampling and the setting for the bin width of the histogram.

2. Coupling between asynchronous motions. When a discrete component of sarcomere lengthening was evident in the histogram of the asynchronously shortening cell, its amplitude was of the same order of magnitude as that associated with the shortening sarcomeres. The amplitudes of the two components were rarely equal, however, with the lengthened component being invariably narrower and, usually, larger in amplitude (*arrows*, Fig. 2 *D*). Because the net length of the cell decreases, the areas subtended by the respective components of the histogram are not equal. In addition, the existence of a slack or viscoelastic coupling between the shortened and lengthened elements would complicate any relation between the separate components at the histogram's extremes. However, if the lengthened elements are elastically coupled to shortening elements, asynchrony should predictably alter the shape of other components of the histograms besides those sampled only at the extremes of shortening and lengthening.

Fig. 3 *A* compares two histograms obtained from a repetitively scanned segment of a cell during separate periods when it shortened first asynchronously and then synchronously, as judged by direct observation of the cell. Asynchrony broadened the central component of the histogram in a nonsymmetrical fashion (Fig. 3 *A*).

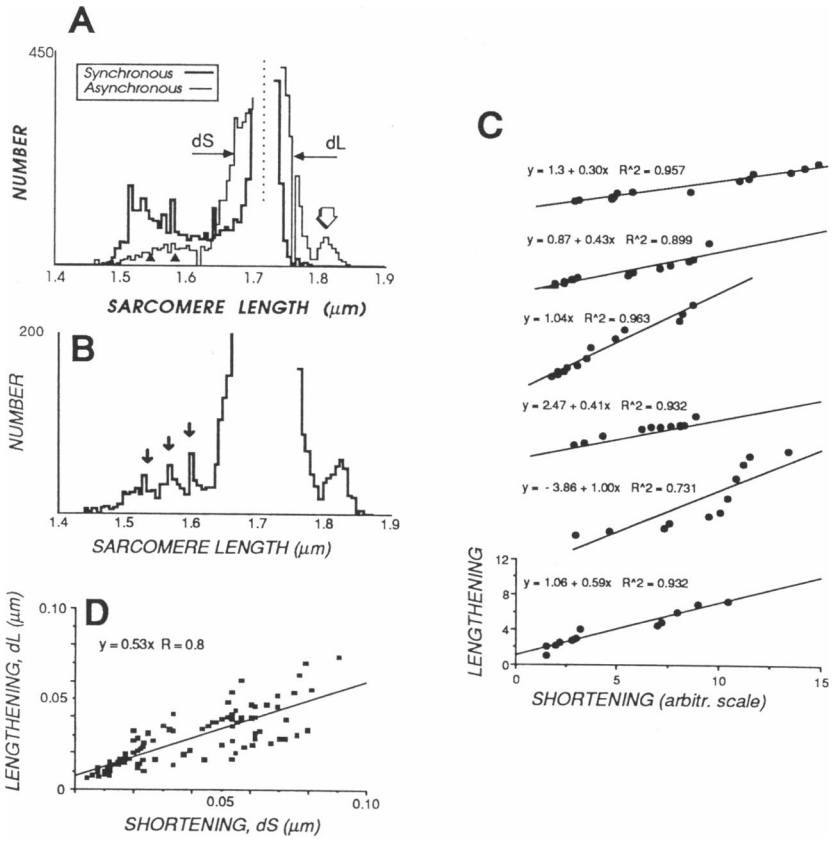

FIGURE 3 Coupling between sarcomere lengthening and shortening in asynchronously contracting myocytes. (*A*) Two histograms of scanned sarcomere lengths in a myocyte that contracted both synchronously (*heavy lines*) and asynchronously (*fine lines*). Comparison at any amplitude of the central portion of the histogram for shortening (d*S*) and lengthening (d*L*) shows that asynchrony broadens the overall distribution asymmetrically. The broad open arrow denotes a population of lengthened sarcomeres. Peak amplitude in both histograms, 900 counts/10,000 samples. (*B*) Example of a histogram from another asynchronously contracting myocyte showing discrete components in the shortening population (*small arrows*). These components cannot be attributed to the isolated peaks or dropouts that represent sampling interactions with the bin settings of the computer display that are evident in *A*. (*C*) Proportionality between small displacements in lengthening and shortening, as inferred from the broadening of the central histogram. The broadening of the histogram due to shortening and lengthening (d*S* and d*L*, respectively as denoted in *A*) was sampled at selected amplitudes in six asynchronously contracting cells. R^2 represents the coefficient of correlation for fit of the data to a linear regression. (*D*) Relations between shortening and lengthening for the combined data in *C* indicates that little internal slack exists since small displacements are well coupled.

Fig. 3 *C* compares the nonsymmetrical distribution of sarcomere length, obtained by measuring the respective components of shortening and lengthening about the mode at various amplitudes of each histogram (e.g., *horizontal arrows* in Fig. 3 *A*). The average slope of the relations between broadening due to lengthening and shortening, obtained by linear regression of histograms from six cells was 0.622 ± 0.29 (SD). (The average of the respective correlation coefficients, R^2, was 0.946 ± 0.045.) The overall proportion between shortening and lengthening about the modal point for all six of the nonsymmetrical distributions of sarcomere length was ~1:0.5, as seen when the data from all histograms were lumped (Fig. 3 *D*). Thus, asynchrony broadens the distribution of sarcomere lengths in a graded manner that is similar for both large and small displacements. Little slack exists between the shortening and lengthening elements at the rest length of the cardiac cell, a fact that is consistent with our premise that the patterns of nonuniformity are transmitted by elastic connections between the striations.

Qualitative aspects of prelengthening

Because the sarcomeres can be extended beyond their initial length in the intact cell, the details of prelengthening reveal information about the properties of structures which connect the sarcomeres. In some (but not most) guinea pig cells asynchronous behavior could be induced repeatedly after a period of electrical stimulation at rapid rate, as shown in Fig. 4. Sarcomere length is sampled in two windows simultaneously that correspond here to fixed regions on the cell. For sake of description, we refer to the window which first samples the wave of contractile activity as the 'leading window', as opposed to the 'trailing window' which samples the subsequent propagated contractile behavior. (The direction of propagation was easily determined by noting the onset of shortening and the time of peak shortening.) As evident in Fig. 4 *A*, the sarcomeres in the trailing window are prelengthened before the arrival of the contractile focus. Second, the sarcomeres in the leading window appear to be over extended during their phase of relaxation by the subsequent shortening in the trailing window. This sequence was complementary: precontractile lengthening and postcontractile overextension occurred in the first and the second window, respectively, when the direction of propagation of consecutive contractile waves spontaneously reverses (Fig. 4 *B*). Synchrony was restored rapidly with the onset of regular stimulation as manifested by contractions showing neither pre- nor postlengthening. This complementary response, plus the absence of prelengthening or postlengthening in the electrical stimulated contractions, demonstrates that the lengthening of the sarcomeres is not due to (*a*) a localized weakness in the cell, nor (*b*) a spurious effect of spatial heterogeneity in fixed point sampling.

Time course and extent of prelengthening

Often the onset of prelengthening and the disappearance of postlengthening are sufficiently discrete to estimate the duration of asynchronous contraction. A representative example is illustrated in Fig. 4 *A*, where the duration of contraction can be estimated to be ~0.96 s. The local velocity of propagation of the spontaneous wave, estimated from the difference in onset of shortening in each window, is ~86 μm/s. Consequently, the net scale of the displacements arising from the spontaneous contraction propagates for 0.96 s × 86 μm/s = 83 μm, or a dimension that approaches the expected length of the isolated cell. Close examination of the sarcomere motions in the respective windows also indicated that prelengthening of the sarcomeres often appeared to begin at the same time in the different regions of the cell.

Fig. 5 shows the course of sarcomere length changes at higher temporal resolution in a separate sequence of spontaneous beatings of the same cell shown in Fig. 4. Each window samples a region that is 4.5 μm in length, where the center-to-center separation of the windows is 7.5 μm. From the 70 ms delay between the onsets of activation in the respective areas, the velocity of propagation of activation can be calculated to be ~100 μm/s. Because prelengthening begins between 0.12 to 0.16 s before activation, the prelengthening of the sarcomere can be estimated to extend ~12 to 16 μm, a value in agreement with an estimate based on qualitative two-

FIGURE 4 Detection of nonuniform motions between sarcomeres in spontaneous asynchronized contractions. (*A*) (*Top*) The stimulator is turned off after regular stimulation (*contractions* at *left*), at which point spontaneous waves of contraction may sometimes occur. Asterisk denotes prelengthening of sarcomeres in the second region that is associated with shortening in the first. The arrow denotes postlengthening of sarcomeres in the first region that is associated with shortening in the second. *T* denotes the period between the appearance of onset of prelengthening in one region and the cessation of postlengthening in the other. (*B*) (*Bottom*) Reversal of pre- and postlengthening which depends upon the direction of propagation of the spontaneous wave of contraction. Prelengthening is denoted by asterisks, and postlengthening is denoted by the small double arrows. Pre- and postlengthening are not seen when spontaneous contractions are synchronized (third contraction), and so lengthening cannot be associated with regional weakness in the cell. The amplitude in asynchronous motions appears reduced in the first window because the area it samples is larger.

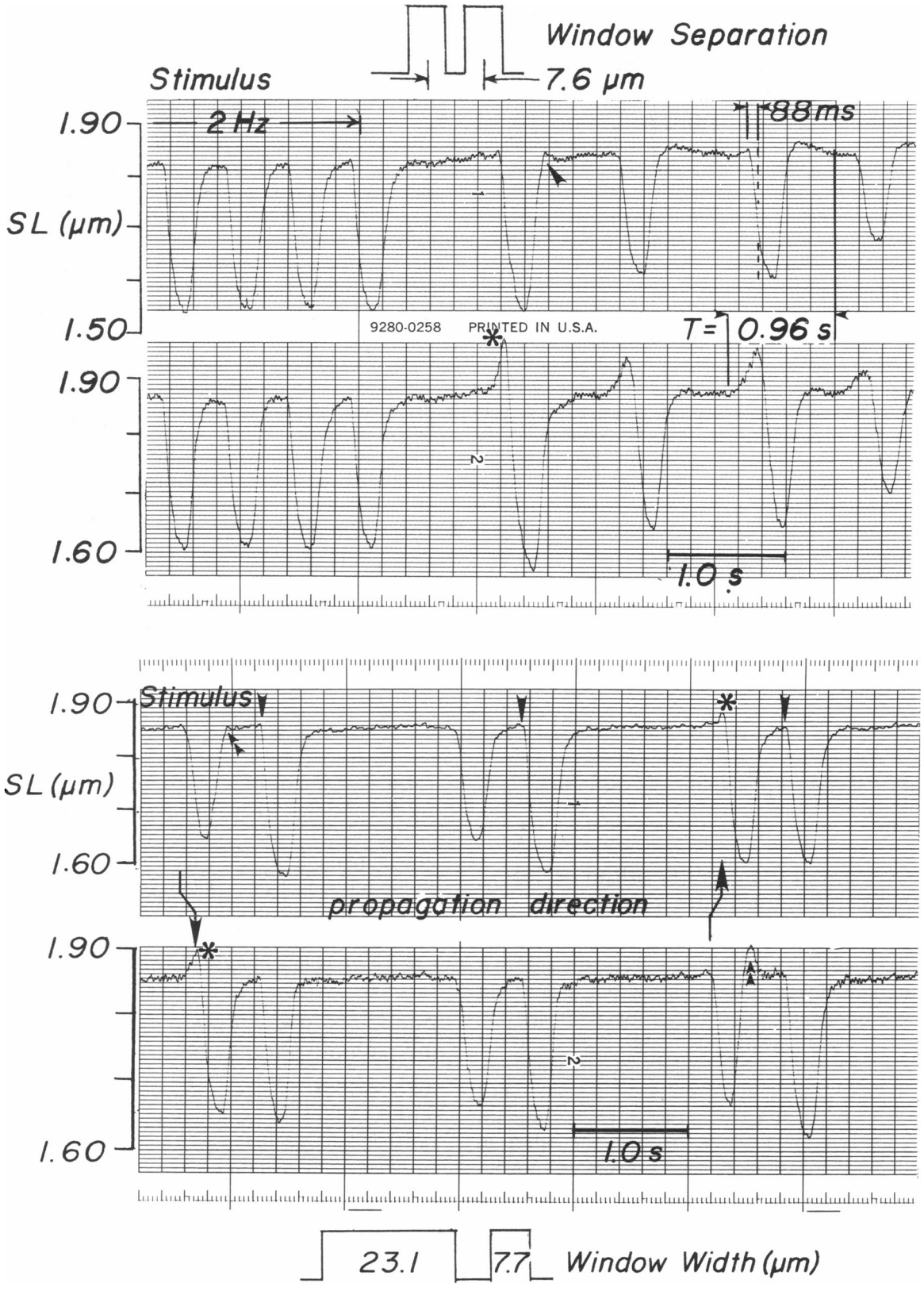
Window Separation
Stimulus
7.6 μm
1.90
2 Hz
88ms
SL (μm)
1.50
9280-0258 PRINTED IN U.S.A.
T= 0.96 s
1.90
1.60
1.0 s
1.90
Stimulus
SL (μm)
1.60
propagation direction
1.90
1.60
1.0 s
23.1
7.7
Window Width (μm)

FIGURE 4

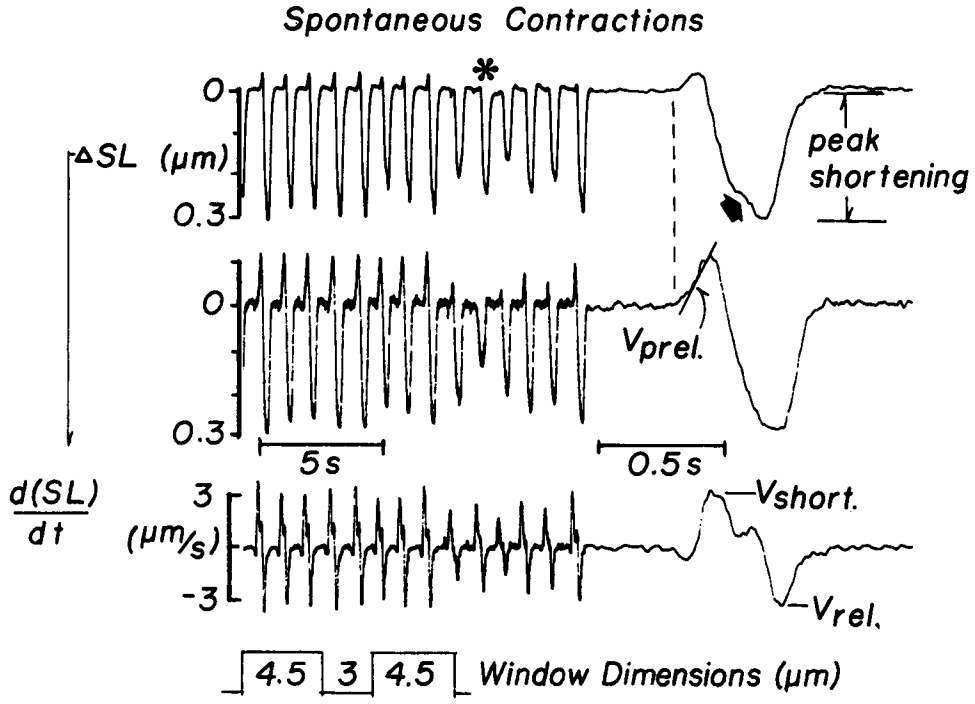

FIGURE 5 Sequence of regular occurring spontaneous contractions induced by touching the cell with the microelectrode. Prelengthening occurs in both regions simultaneously, and is thus distributed along the length of the cell in advance of the arrival of the contractile wave. V_{prel}, V_{short}, and V_{rel}, denote the respective maximum velocities of prelengthening, shortening, and relengthening, as analyzed in Figs. 7 and 8. The broad arrow denotes a common disturbance near the peak of asynchronous shortening that can also be observed upon close inspection of Figs. 4 and 5. *Fairly synchronous contraction as was determined from a higher resolution chart recording. $d(SL)/dt$ denotes the velocity of the sarcomere motions in the first window.

dimensional displays of nonuniformity such as shown in Fig. 2 *C*.

Establishment of the cellular origin of the force that prelengthens the sarcomere

The observation that sarcomeres can be extended beyond their initial length in the intact cell indicates that shortening sarcomeres generate force, but it does not resolve where the force arises that resists their shortening. The cells are attached only weakly, if at all, to the substrate, since they can be easily displaced by a micropipet. (In this case, they tend to rotate about a point; i.e., only a very restricted attachment that would not account for prelengthening.) However, because the effect of prelengthening is distributed, it is necessary to rule out whether prelengthening represents an unsuspected interaction between the cell and the substrate. Prelengthening occurred when the coverslip forming the bottom of the observation chamber was siliconized (17) to minimize any residual mechanical interaction between the cell and the substrate. Fig. 6 illustrates an experiment in which the cell was lifted 50–60 μm from the bottom of the observation chamber by a suction micropipet. The suction was adjusted so that the striations appeared straight to minimize any effect that the pipet might have on the cell's mechanics. The fact that prelengthening of the sarcomeres remains associated with asynchronous contraction (Fig. 6) demonstrates that a force which sustains prelengthening arises within the cell.

Dynamics of sarcomere prelengthening in the asynchronously contracting cell

As is evident in Figs. 4, 5, and 6, the magnitude of prelengthening in asynchronous contraction is highly variable. In any cell, the degree of prelengthening might be affected by many factors such as: the degree and velocity of sarcomere shortening; the direction of propagation of the contractile wave; the velocity of propagation of the contractile wave; the synchrony of contraction; and the resistance of the sarcomeres to prelengthening.

To learn more about the mechanical properties of the

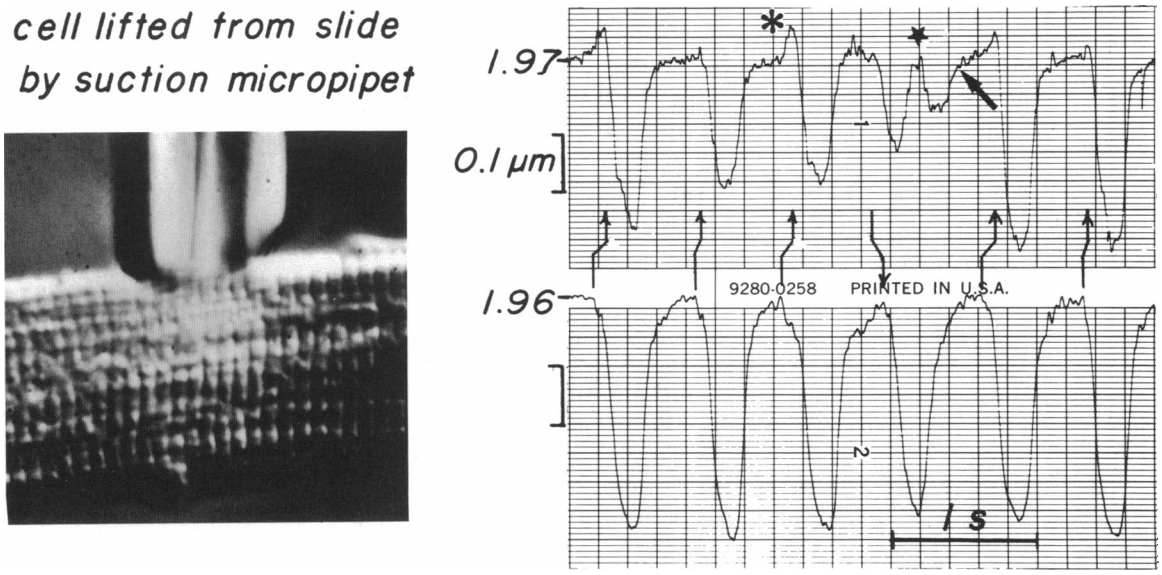

FIGURE 6 The force that prelengthens sarcomeres originates in the cell. The panel at left shows the appearance of the striations in a myocyte that was lifted from the surface of the microscope chamber by a suction micropipette. The sarcomere motions in this region is shown at right. Prelengthening is denoted by the asterisk, while the direction of propagation of the contractile wave is indicated by the bent arrows. The large arrow indicates one contraction where the duration of the spontaneous shortening is prolonged by stretch (*star*) of the sarcomeres by contraction in the neighboring region. Window widths, 6 μm.

structure(s) that sustains prelengthening, we analyzed in detail the sarcomere motions in cells where spontaneous contractions could be reproducibly induced by touching the cell with the stimulus pipet, while a separate sequence of uniform contractions could be elicited afterward by electrical stimulation. The relation between the respective measurements from one such cell is shown in Fig. 5. Peak shortening was recorded in the leading window as the difference between the 'rest' length and sarcomere length at peak shortening. The peak velocities of sarcomere shortening and relengthening were determined by electronic differentiation of the sarcomere length signals in the leading window. Prelengthening was determined in the trailing window as the difference between the rest length and the sarcomere length at the onset of shortening. The maximum velocity of prelengthening in the trailing window was determined by eye. The data were examined in only those paired asynchronous spontaneous contractions in which the onset of shortening in the leading window preceded that in the trailing window by 0.1 to 0.2 s: data from spontaneous waves propagating in the reverse direction was discarded. The width of both windows was 4.5 μm and they were separated by a gap of 3 μm, while the space between the windows was positioned to overlie the central, nontranslating portion of the cell. Data was recorded from 64 spontaneous, sequential contractions and is plotted in Fig. 7.

Subject to these definitions, the amount of prelengthening correlated well with the extent of peak shortening in the advancing contractile wave (Fig. 7*A*). The maximum velocity of shortening increases as well with peak shortening, but beyond a critical level of ~3 μm/s both prelengthening and shortening were unrelated to increments in the velocity of shortening (Fig. 7*B*). The fact that of prelengthening is proportional to shortening in the advancing wave of contraction supports our working hypothesis that sarcomere lengthening is sustained by elements within the cell which behave elastically. Any force due to viscoelasticity ought to be proportional to the velocity of prelengthening, and the latter is seen to increase progressively as the contractile wave approaches (Figs. 4*A* and 5). If elements that are located in series with the shortening sarcomeres are viscoelastic, however, we would expect that prelengthening would depend upon the velocity of their 'prestretch' even after corrections are made for elastic interactions. By this rationale, any viscous resistance ought to be reflected in a dependence of the extent of prelengthening upon the velocity of 'prestretch' when the former is normalized by sarcomere shortening in the leading window. As shown

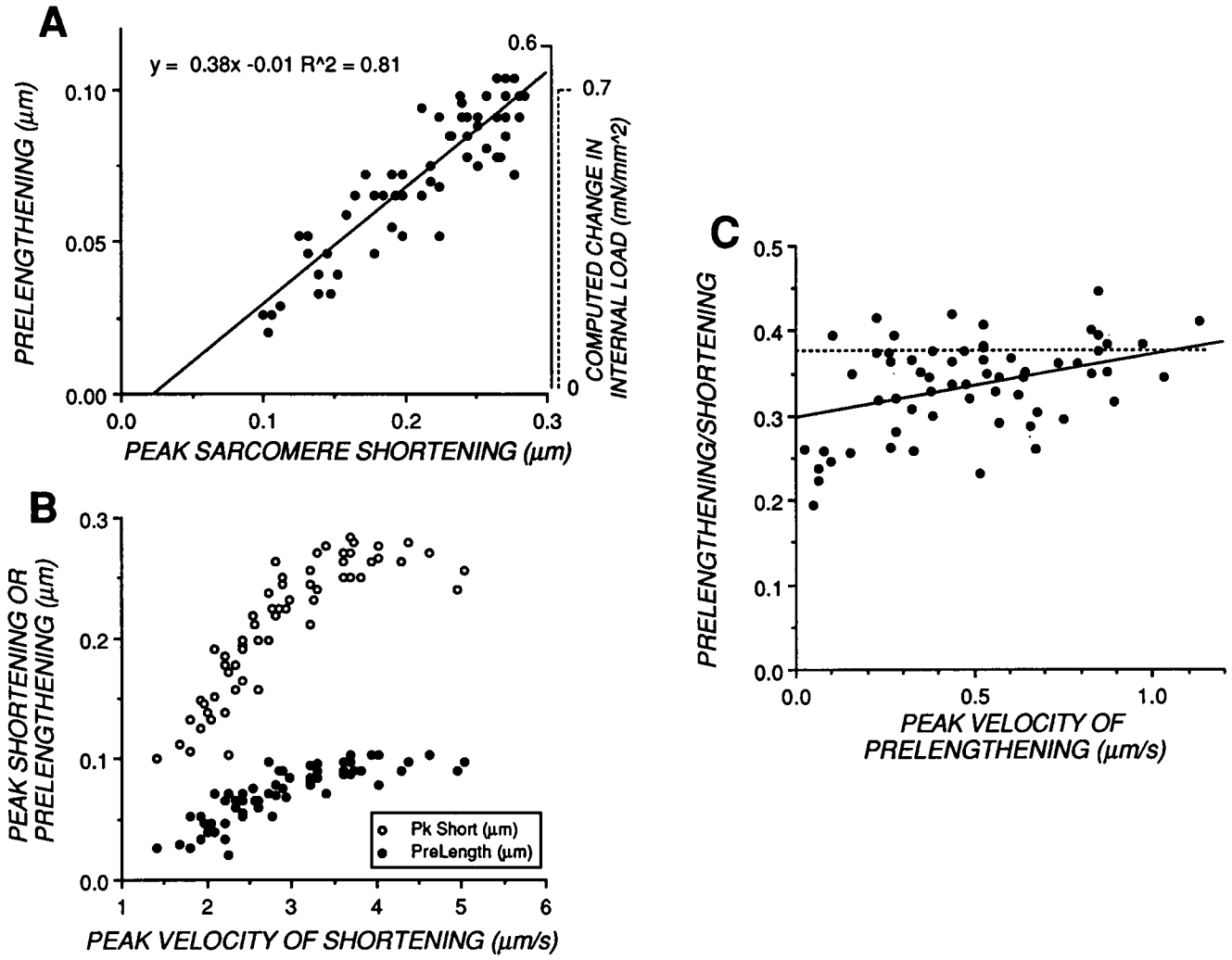

FIGURE 7 Dynamics of asynchronous motions between sarcomeres. (*A*) Dependence of prelengthening upon shortening in the advancing contractile wave. (*B*) Influence of the velocity of sarcomere shortening in the advancing wave on prelengthening and peak shortening. (*C*) Lack of influence of the velocity of lengthening of the sarcomeres upon prelengthening when the latter is normalized by the peak shortening in the advancing contractile wave. The solid line represents the linear regression which shows no correlation. The dashed line indicates the ratio of prelengthening to shortening (0.38) that was determined by linear regression in *A*. Refer to Fig. 5 for definition of measurements, and to text for discussion of scales estimating internal load in *A*.

in Fig. 7 *C*, there is little indication that prelengthening is influenced by viscous interactions.

Comparison of sarcomere dynamics in synchronous and asynchronous contractions

Further information about the influence of the asynchronous motions can be obtained by asking how such motions compare with the dynamics of the sarcomere in the uniformly contracting cell? Fig. 8 contrasts the dynamics of the uniformly contracting cell with the data from the spontaneous asynchronous contractions presented in Fig. 7. The maximum velocities of shortening and relengthening were recorded in sequential contractions under both conditions, as shown in Fig. 8 *A*. The beat-to-beat variability that characterized the velocity of shortening and relengthening in the spontaneous contraction was immediately reduced by the onset of electrical stimulation (Fig. 8 *A*).

The forces causing prelengthening should slow the velocity of shortening and speed the velocity of relengthening: i.e., any additional elastic internal load that arises from nonuniform contraction would reduce the ratio of

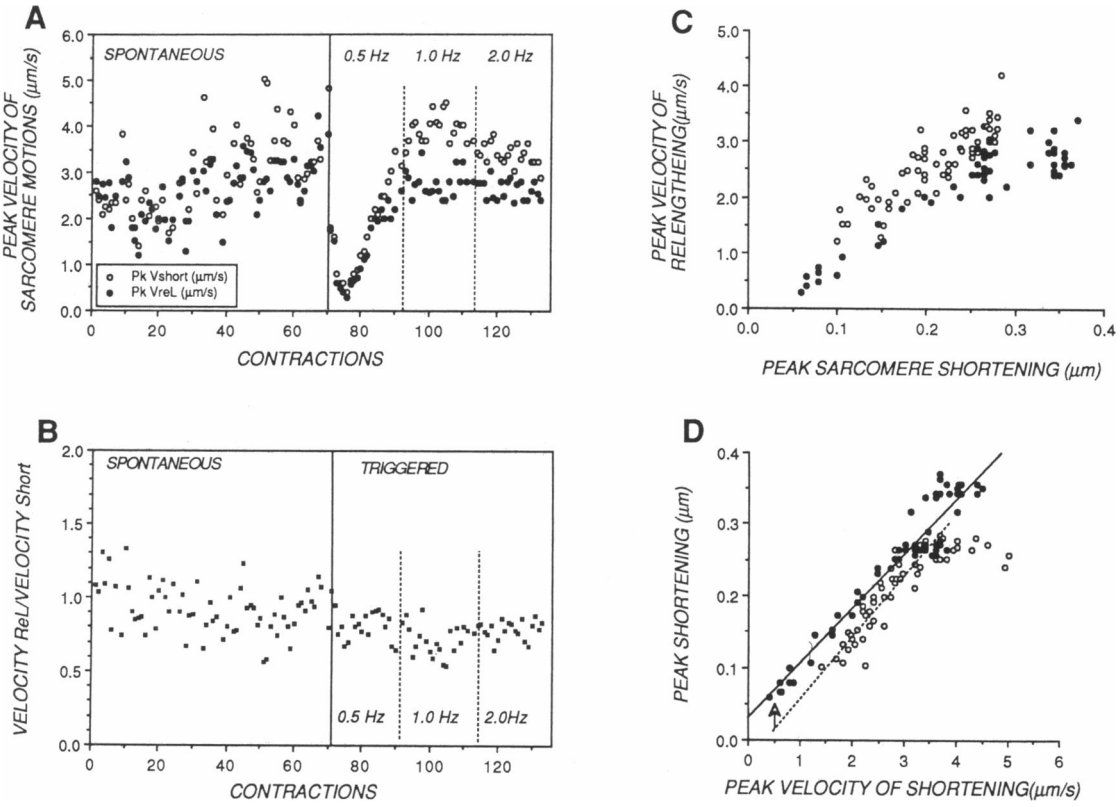

FIGURE 8 Comparison of sarcomere dynamics in asynchronous contractions and uniform, electrically triggered contractions. (*A*) Variation of the velocity of shortening and lengthening motions in a sequence of spontaneous and triggered contractions. The relation between shortening and relengthening motions is more reproducible with the onset and adjustment to electrical stimulation as shown at right. (*B*) The ratio of the respective velocities of relengthening and shortening as measured in consecutive contractions. The ratio of relengthening to shortening velocities is 0.924 ± 0.17 (±SD, $N = 64$) in the spontaneous contractions and 0.772 ± 0.10 (±SD, $N = 62$) in the triggered contractions. The difference is statistically significant so that, relative to shortening, the sarcomeres relengthen more slowly when contraction is synchronous. (*C*) Comparison of the effect of peak shortening upon the velocity of sarcomere relengthening in synchronous (*solid symbols*) and asynchronous (*open symbols*) contractions. Asynchrony tends to enhance relengthening at any sarcomere length. (*D*) Relative to the peak velocity of shortening, peak shortening is reduced in the asynchronous contractions (*open symbols*). The solid line and the equation represents fit of the data in synchronous contractions (*solid symbols*) to a linear regression.

the two. Thus, in both synchronized and asynchronized contractions, the ratio of the respective velocities of the relengthening and shortening was less variable than the absolute values of either parameter, as seen in Fig. 8 *B*. The average ratio of the velocity of relengthening to shortening was 0.924 ± 0.17 (±SD, $N = 64$) in the asynchronous spontaneous contractions and 0.772 ± 0.10 (±SD, $N = 62$) in the uniform contractions in which the cell was stimulated at rates that spanned that of the spontaneous activity. The difference between the respective ratios was statistically significant ($P < 0.0001$, students paired t test; cf. 24).

These results support the idea that asynchrony creates an additional internal force in the isolated cell, but a comparison of changes in the ratio of velocities does not reveal its magnitude. However, any elastically-stored compressive force within the shortened sarcomere ought to be the same at any length regardless of whether the cell contracted synchronously or asynchronously. Thus, any such additional force would (*a*) add to the restoring force which relengthens the shortened sarcomere, and (*b*) decrease the amount of sarcomere shortening. In fact, relative to any length, relengthening appears to be ~0.5 μm/s faster in asynchronous contraction (Fig. 8 *C*). Conversely, relative to the velocity of shortening, peak shortening is reduced by ~0.05 μm (Fig. 8 *D*).

DISCUSSION

We have used two different methods to characterize the nonuniform motions that occur in the asynchronously

contracting heart cell. Both methods indicate that (*a*) sarcomeres are transiently lengthened in a nonuniform fashion for a region extending approximately 10 to 15 μm in the unattached cell, and (*b*) that the inactive sarcomeres are elastically coupled with little internal slack. Extension of the inactive elements in the unattached cell reflects an intracellular force, and this parallels an effect of asynchrony on the dynamics of the active elements. The additional force created by asynchronous prelengthening of the inactive elements acts in consort with the intrinsic restoring force that normally arises within the myofibril. Consequently, prelengthening has two separate implications for the mechanical nature of the cardiac cell: (*a*) its amplitude allows us to estimate the magnitude of the intrinsic restoring force in the intact cell; and (*b*) its nonuniform distribution provides insight about the connections between the cardiac sarcomeres. Others have inferred that the sarcomere can be stretched from the localized transmittance of the unattached cell (3). However, the biphasic fluctuation in transmittance (cf. 3) looks appreciably different from that we find for sarcomere motion.

Interpretation of dynamics of sarcomere motions by repetitive scanning of the point of sampling

The interpretation of conventional observations made by sampling at a fixed position requires that sarcomere length within the sample remains reasonably uniform. In this case the mean length of the population can be observed with high temporal resolution (18), and the synchrony of motion can be determined by sampling at a second site on the cell (10). Alternatively, the point of sampling can be restricted to a few elements and displaced in a controlled manner. Temporal resolution is sacrificed for a statistical treatment in the latter method, but spatial resolution can be applied to one-to-two striations.

The distinction becomes clear when inferring the basis for the shape of the histogram, whose amplitude represents the relative incidence of striations existing at any length during the sampling period. Thus, the characteristic sharp peak of the shortest components of histograms from the synchronously contracting cell (Fig. 3 *A*) reflects the fact that the velocities of both shortening and relengthening slow at short lengths (14) and that peak shortening is uniform. However, the histograms from asynchronously shortening cells showed just the opposite morphology (Figs. 2 *D* and 3 *B*), in that the amplitude of the component in shortening was weak and broadly distributed. Histograms from some asynchronously shortening cells showed multiple subpeaks in the shortening components, but here too their respective amplitude decreases at shorter lengths (Fig. 3 *B*). Thus, the peak shortening of individual sarcomeres must be nonuniform during asynchronous contraction, and/or the velocity of their motion must depart from a simple length-dependence (cf. *arrow,* Fig. 5 *A* and later discussion). In contrast, the component of the histogram representing the prelengthened elements was always discrete, as might be expected if the velocity of their passive lengthening was slow and/or their resistance to extension increased with stretch.

Asynchronous sarcomere mechanics

Asynchrony has long been evoked as an explanation for various patterns of altered contraction in the heart. However, we are unaware of any prior study where the mechanics of asynchrony could be interpreted by itself, i.e., free from uncertainties due to application of external forces.

Observation of individual striations in asynchronously contracting heart cells have found that the velocities of shortening and relengthening appear constant (16), a behavior that would result in a 'triangular' pattern of shortening and relengthening. We have never observed this pattern of shortening in synchronized contractions (8, 10, 13, 14). However, the reversibility in the dynamics of the sarcomere in contiguous contractions show that asynchrony could make the velocity of both shortening or relengthening appear more constant. Specifically, this is evident in the first spontaneous contraction in the top trace and the last spontaneous contraction in the bottom trace of Fig. 4 *B*. The reversal of this behavior in the same sarcomeres suggests that velocity would appear more constant if the early shortening is slowed due to an additional force caused by stretch of the adjacent region, while the velocity of relengthening would appear more constant if the sarcomeres are forcibly relengthened. Thus, a triangular pattern of shortening and relengthening (16) is consistent with the existence of an additional intracellular load on the sarcomere when contraction is asynchronous.

The time course of the sarcomere's motions also supports the existence of an additional intracellular force in asynchrony. Cross-bridge formation sensitizes the myofilaments to calcium (21), an effect that should prolong activation. In Fig. 6 the timing of spontaneous events is such that one contraction which is detected in the trailing window interrupts the shortening in the preceding region. The interrupted contraction is prolonged, for the sarcomeres reshorten as the adjacent sarcomeres relengthen. (The effect is analogous to the behavior of strong and weak sarcomeres in series [12].) The occurrence of delayed, nonpropagated, additional shortening has another significance. Because a parallel

contraction is not seen in the adjacent window, the frequency of shortening cannot be used to measure the incidence of a local rise in myoplasmic calcium concentration!

A close inspection of the experimental records reveals a transient slowing and reacceleration of motion occurs prior to peak shortening (cf. *arrow,* Fig. 5*A*; fifth contraction of the top trace in Fig. 4*A*). The transient slowing of the shortening in the leading focus is also consistent with an increased load transmitted by prestretch in the adjacent trailing region. As activation advances to the trailing region, active shortening should abolish the load that prestretch imposes upon its neighbors, and shortening in the leading region should accelerate briefly (as is seen). Interrupted shortening (Fig. 6) may simply represent the extreme case of the long range coupling between sarcomeres.

The preceding motions, observed by sampling sarcomere length in neighboring regions of the cell, appear to be fully consistent with the motions deduced previously from the histograms obtained by scanned sampling. The precise temporal associations represent a distributed effect of the propagated wave of contraction, but it is unlikely that these dynamic events represent an artifact of sampling specific sarcomeres, per se. Peak shortening and prelengthening are coupled for both large and small displacements, so that their measurement provides a valid indication of the mechanical couplings in the cell.

Prelengthening and the estimation of the internal load in the asynchronously contracting, intact cardiac cell

Because the shortening and prelengthening sarcomeres are in mechanical equilibrium, we sought to estimate the net force exerted by the shortened sarcomeres. Specifically, the extensibility of intact (6), detergent-treated (2), or mechanically dissected (5, 7) heart cells is generally known, and so the magnitude of the force exerted by the shortening focus can be gauged by the strain imposed on the prestretched region. As an estimate of the force which sustains prelengthening, Fig. 7*A* illustrates a scale that was computed by assuming that the extensibility of the guinea pig cell is of the same order of the extensibility of single hamster myocytes (6). Thus, the increase in force exerted by the shortening sarcomeres can be calculated as $\exp^{KE} - 1$, where K is the stiffness constant (7.48) and E is the strain ($dL/L_{initial}$) imposed on the stretched elements (6). If the resistance to stretch in our intact cells resembles that measured in the hamster myocyte (6), it can be readily seen that sarcomere's additionally generate ~0.3–0.5 mN/mm^2 during asynchronous contractions (Fig. 7*A*).

A recent study introduced a means to compute the resistance to stretch in the detergent-treated guinea pig myocyte directly from the length-dependence of a dynamic modulus of its elasticity (2). Based on the effect of length on the modulus of elasticity, $E(SL)$, the length-dependence of passive stress, σ, can be computed as $\sigma(SL) = [E(SL) - 6.676]/4.17$, where $E(SL)$ was determined to be $E(SL) = [\exp^{2.996(SL)}]/44.39$ (all equations and constants obtained from reference 2, Tables 2 and 3). Considering rest length of the sarcomere to be 1.9 μm, it can be computed that prelengthening of 0.1 μm should require a force of 0.56 mN/mm^2 for a cylindrically shaped myocyte. Use of a rectangular cross section would augment this estimate by 1.3 fold (2), giving an upper limit to the estimated prelengthening force of 0.7 mN/mm^2. The range of these estimates is illustrated also in the dashed scale Fig. 7*A*.

Because prelengthening is limited by the arrival of a contractile wave, the magnitude of the additional force we attribute to nonuniform lengthening may be underestimated. Any viscoelastic resistance to stretch would increase the force generated by the prelengthened elements. The effect, however, is likely negligible: the velocity of prelengthening is small; it does not alter the relation between the extent of prestretch and peak shortening (Fig. 7*C*); and a comparable coupling between shortening and lengthening is seen for small displacements where any putative viscoelastic resistance to extension would certainly be minimal (Fig. 3*D*).

Direct visualization of the spontaneous wave of myoplasmic calcium in guinea pig myocytes (24) reveals that its free ion concentration is not transiently lowered during that phase when we also find that the sarcomeres can be extended beyond their 'rest' length (i.e., postlengthening). The existence of postlengthening also indicates that an additional internal force is generated by asynchrony, although we cannot gauge its effect because of falling activation. A direct correlation between myoplasmic calcium and sarcomere length in intact and skinned guinea pig myocytes (23) suggests that an initial sarcomere length of 1.8 μm reveals preactivation by ~100 nM myoplasmic [Ca^{+2}]. Preactivation, however, would only serve to increase the resistance to prelengthening and thus amplify any additional force revealed by asynchronous lengthening.

Implications for the involvement of the cell in diastolic recoil

The magnitude of the force that generates prelengthening remains an estimate because the extensibility of the myocyte was not measured. Even at a low value of 0.5 mN/mm^2, the internal force that resists asynchronous shortening in the isolated cell (Fig. 7) appears to be of the same order as the 1–2% level of force which is

sufficient to markedly accelerate relengthening in isolated heart muscle (25). The fact that its cells buckle when external relengthening is slowed in the multicellular isolated muscle preparation (9) implies that the elastic properties of the cell determine the rest length of cardiac muscle. Unattached cells produce little force, but early relengthening of the fibers of the heart can occur at comparably low forces. A very simple model of the ventricle indicates that a force of only 0.5 mN/mm^2 would be sufficient to create negative intraventricular pressures of ~10 mmHg (8).

The cell's true restoring force must be larger than any estimate based upon the extrinsic force that sustains prelengthening, because the latter reveals only the net force produced by the actively shortening sarcomeres. Fig. 9 illustrates a simple model of the mechanical interaction between an actively shortened and passively lengthened segment of the isolated cell. By this reasoning, the active force generated by the myofilaments (F_{myo}) in the shortening sarcomeres is balanced by an intrinsic myofibrillar compressive force (F_{comp}). The resultant net force is in equilibrium with an extrinsic force due to the prelengthened sarcomeres (F_{prel}), and a differential force due to a component of hydrostatic pressure (P) transmitted by the cross sectional area (A) of the cell. The influence of a hydrostatic pressure gradient can be assumed to be small, however, because (*a*) neither internal dialysis of the cell (15) nor exposure to detergent (10) shortens the initial sarcomere length, and (*b*) any effect of pressure would be further reduced by the ratio of the cross sectional areas by a factor ($[1 - L_s/L_l] = 0.2$), where L_s and L_l represent the lengths of the shortened and lengthened elements, respectively. Consequently, the balance of forces between the segments can be approximated as

$$F_{myo} - F_{comp} = F_{prel},$$

and the relative force produced by the active interactions between the myofilaments can be treated as

$$F_{myo}/F_{max} = (F_{comp} + F_{prel})/F_{max}.$$

Velocity of shortening is exquisitely sensitive to the small increments in tension produced by the unattached cell due to the hyperbolic shape of the force-velocity relation in muscle. Regardless of the true magnitude of the extrinsic force generated by asynchrony, F_{prel}, its very small effect, if any, on the depression of the velocity of shortening indicates that the intrinsic restoring force, F_{comp}, must be *appreciably larger* than 0.5–0.7 mN/mm^2.

The preceding interpretation does not require that a restoring force is elastically coupled to the length of the shortened sarcomere, but it does assume that the altered dynamics reflect a restoring force rather than an uncertain effect of myoplasmic calcium [ion]. Conversely, a length-dependent elastic restoring force has been inferred from the peak velocity of relengthening in guinea pig myocytes when relaxation is triggered by liberation of caged ATP in the absence of calcium (19). Considering a cylindrical cell 20 μm in diameter, cellular restoring forces chosen to support the latter model (250 to 800 nN; Fig. 3, reference 19) would give rise to a maximum restoring force of 0.8 to 2.5 mN/mm^2. However, the peak velocity of relengthening reported for ATP-triggered relengthening (0.77 ± 0.13 μm/s, reference 19) is only one third the value of 2.5 μm/s (Fig. 8 *A*) that we find for the synchronous contraction in which relengthening is likely governed by calcium reuptake in the presence of ATP. As the presence of residual ADP may slow relengthening (see comments from reference 19), the maximum restoring force would be larger than that

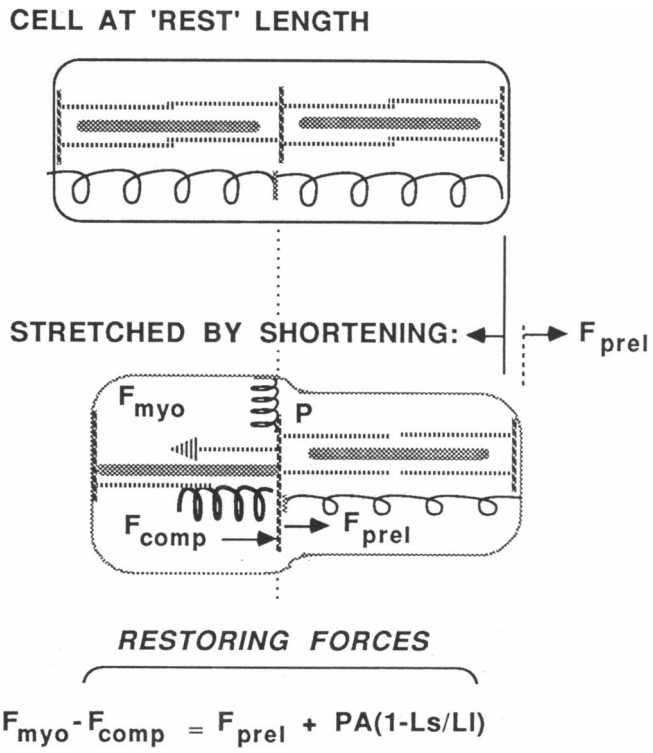

FIGURE 9 An explanation of forces underlying relengthening in the asynchronously contracting, unattached cell. The active force generated by the myofilaments in the shortening sarcomeres (F_{myo}) is balanced by a myofibrillar compressive force (F_{comp}), a force due to the prelengthened sarcomeres (F_{prel}) and a differential force due to a component of hydrostatic pressure (P) transmitted by the cross sectional area (A) at ends of the cell. Any influence of the hydrostatic pressure, assumed to be small, is reduced further by the ratio of the respective cross sectional areas by a factor ($[1 - L_s/L_l] = 0.2$), where L_s and L_l are the respective lengths of the shortened and lengthened sarcomere. Refer to text for details.

inferred. Thus, the latter finding (19) is also in general accord with our expectation.

Structures that transmit the prelengthening force

We have shown that the force that sustains prelengthening arises within the cell (Fig. 6). Passive lengthening extends nonuniformly over a region of ~10 to 15 μm, and so the structures that resist this extension must extend over a comparable range. Two distinct mechanisms can be advanced for nonuniform prelengthening in the unattached cell. First, the sarcomeres might be under slight compression by longitudinal elements that parallel the sarcomere. In this scheme, partial shortening in the length of the cell reduces tension in these elements elsewhere, an event that decompresses the sarcomere to permit their lengthening (Fig. 9). This requires long range tethering by elements that are not connected to contiguous striations, which would then be disposed outside of the myofibril. A second requirement of this scheme is that tension on these elements would have to be imposed by a restoring force that arises after the subsequent assembly of the contractile lattice. Alternatively, the resting sarcomeres could be under an initial tension that is created by an internal hydrostatic force which extends the entire resting cell. However, an initial hydrostatic extension of the sarcomere seems unlikely for reasons discussed previously. Active extrusion of organelles by shortening of myofibrils and transient active hydrostatic pressure gradients might extend the inactive sarcomere, but these mechanisms do not provide a simple explanation for why the prelengthening is localized nor why shortening can be transiently slowed (cf. *arrow*, Fig. 5 *A*). Moreover, in preliminary observations we have also found that localized lengthening can be induced in a detergent treated cell which is locally activated by calcium iontophoresis.

Whether an intracellular parallel elasticity originates within the myofibril or in its surrounding structure cannot be distinguished when strain is uniform along the length of an isolated cell. Multiple sources of a parallel elasticity likely exist within the cell, and the actual interconnections between the striations and the cardiac cytoskeleton have not been mapped. As the various components of the cell should have different elastic properties, the patterns of strain imposed by nonuniform activation would unmask the differential nature of tethering between the striations. The observations that prelengthening (*a*) is nonuniform, (*b*) its extent is limited, (*c*) it is proportionately coupled to active shortening elsewhere by (*d*) a seemingly elastic mechanism, are all simplest to explain if the tension is passively transmitted by a branched network that does not connect to contiguous striations (Fig. 9, *top*). If such a longitudinally disposed cytoskeleton network also participates in intracellular transport, it would constitute a simple extramyofibrillar mechanism by which the cell transduces the effect of nonuniform external forces into a directed adaptive response.

We thank Mrs. Nadine Stram and Dr. Hong Zhang for technical assistance. The test grating was constructed with the assistance of Mr. R. C. Tiberio at the National Nanofabrication Facility which is supported by the National Science Foundation under grant ECS-8619049, Cornell University and Industrial Affiliates. We also thank Drs. Douglas Christensen (University of Utah) for advice and Ernst Niggli (Berne) for comments. Supported, in part, by HL-21325.

Received for publication 13 May 1991 and in final form 3 September 1991.

REFERENCES

1. Berlin, J. R., M. B. Cannell, and W. J. Lederer. 1989. Cellular origins of the transient inward current in cardiac myocytes. *Circ. Res.* 65:115–126.
2. Brady, A. J. 1991. Length dependence of passive stiffness in single cardiac myocytes. *Am. J. Physiol.* 260 (*Heart Circ. Physiol.* 29):H1062–H1071.
3. Capogrossi, M. C., and E. G. Lakatta. 1985. Frequency modulation and synchronization of spontaneous oscillations in cardiac cells. *Am. J. Physiol.* 248:H412–H418.
4. Fabiato, A., and F. Fabiato. 1976. Dependence of calcium release, tension generation and restoring forces on sarcomere length in skinned cardiac cells. *Eur. J. Cardiol.* 4(suppl):13–27.
5. Fabiato, A., and F. Fabiato. 1979. Myofilament generated tension oscillations during partial calcium activation and activation dependence of the sarcomere length-tension relation. *J. Gen. Physiol.* 72:667–699.
6. Fish, D., J. Orenstein, and S. Bloom. 1984. Passive stiffness of isolated cardiac and skeletal myocytes in the hamster. *Circ. Res.* 54:267–276.
7. Iwazumi, T. 1989. Mechanics of the sarcomere. *In* Cardiac Mechanics and Function in the Normal and Diseased Heart. M. Hori, H. Suga, J. Baan, & E. L. Yellin, editors. Springer-Verlag, Tokyo. 13–22.
8. Krueger, J. W. 1989. Rapid relengthening in isolated cardiac cells and the origin of diastolic recoil. *In* Cardiac Mechanics and Function in the Normal and Diseased Heart. M. Hori, H. Suga, J. Baan and E. L. Yellin, editors. Springer-Verlag, Tokyo. 23–34.
9. Krueger, John W. 1990. Internal buckling reveals the cellular origin of restoring forces in cardiac muscle. *Circulation.* 82:II 162*a*. (Abstr.)
10. Krueger, J. W., and A. Denton. High resolution measurements of sarcomere dynamics and uniformity in cardiac muscle cells. *Biophys. J.* 61:129–144.
11. Krueger, J. W., A. Denton, G. Siciliano, and R. C. Tiberio. 1989. Resolution and Evaluation of asynchronous motions between sarcomeres in cardiac muscle cells. *Biophys. J.* 55:268*a*. (Abstr.)

12. Krueger, J. W., and S. Farber. 1980. Sarcomere length 'orders' relaxation in cardiac muscle. *Eur. Heart J.* 1(suppl A):37–47.

13. Krueger, J. W., D. Forletti, and B. Wittenberg. 1980. Uniform sarcomere shortening behavior in isolated cardiac muscle cells. *J. Gen. Physiol.* 76:587–607.

14. Krueger, J. W., B. London, and G. Siciliano. 1988. Separability of relaxation indices in isolated ventriculocytes. *In* Biology of Isolated Adult Cardiac Myocytes, Wm. A. Clark, R. S. Decker, and T. K. Borg, editors. Elsevier Science Publishing Co., Inc. New York. 406–409.

15. London, B., and J. W. Krueger. 1986. Contraction in voltage-clamped, internally perfused single heart cells. *J. Gen. Physiol.* 84:475–505.

16. Lundblad, A., H. Gonzalez-Serratos, G. Inesi, J. Swanson, and P. Paolini. 1986. Patterns of sarcomere activation, temperature dependence, and effect of ryanodine in chemically skinned cardiac fibers. *J. Gen. Physiol.* 87:885–905.

17. Manniatis, T., E. F. Fritsch, and J. Sambrook. 1982. Molecular Cloning—A Laboratory Manual. Cold Spring Harbor Laboratory. 437–439.

18. Myers, J., R. Tirosh, R. C. Jacobson, and G. H. Pollack. 1982. Phase locked-loop measurement of sarcomere length with high time resolution. *I.E.E.E. Trans. BioMed. Eng.* 29:463–466.

19. Niggli, E., and W. J. Lederer. 1990. Restoring forces in cardiac myocytes. Insight from relaxations induced by photolysis of caged ATP. *Biophys. J.* 59:1123–1135.

20. Reiser, G., R. Sabbadini, P. Paolini, M. Fry, and G. Inesi. 1979. Sarcomere motion in isolated cardiac cells. *Am. J. Physiol.* 236:C70–C77.

21. Ridgway, E. B., A. M. Gordon, and D. A. Martyn. 1983. Hysteresis in the force calcium relation in muscle. *Science (Wash. DC).* 219:1075–1077.

22. Roos, K. P., and A. J. Brady. 1982. Individual sarcomere length determination from isolated cardiac cells using high-resolution optical microscopy and digital image processing. *Biophys. J.* 40:233–244.

23. Siri, F. M., J. W. Krueger, C. Nordin, Z. Ming, and R. S. Aronson, RS. 1991. Depressed intracellular calcium transients and contraction in myocytes from hypertrophied and failing guinea pig hearts. *Am. J. Physiol.* 261 (*Heart Circ. Physiol.* 30): H514–H530.

24. Takamatsu, T., and W. G. Wier. 1990. Calcium waves in mammalian heart: quantification of origin, magnitude, waveform, and velocity. *FASEB J.* 4:1519–1525.

25. Ter Keurs, H. E. D. J., W. H. Rijnsburger, and R. van Heuningen. 1980. Restoring forces and relaxation in rat cardiac muscle. *Eur. Heart J.* 1(suppl A):67–80.

26. Zar, J. H. 1984. Biostatistical Analysis. 2nd ed. Prentice Hall, Inc. Englewood Cliffs, NJ. 196–198.